Title

Integrin-Associated Complexes Form Hierarchically with Variable Stoichiometry in Nascent Adhesions

Journal

Current Biology, 24(16)

ISSN

0960-9822

Authors

Bachir, Alexia I
Zareno, Jessica
Moissoglu, Konstadinos
et al.

Publication Date

2014-08-01

DOI

10.1016/j.cub.2014.07.011

Published in final edited form as:
Curr Biol. 2014 August 18; 24(16): 1845–1853. doi:10.1016/j.cub.2014.07.011.

Integrin-Associated Complexes Form Hierarchically with Variable Stoichiometry during Nascent Adhesion Formation

Alexia I. Bachir[1,*], **Jessica Zareno**[1], **Konstadinos Moissoglu**[2], **Edward Plow**[3], **Enrico Gratton**[4], and **Alan R. Horwitz**[1]

[1]Department of Cell Biology, University of Virginia, Charlottesville, VA 22908 USA

[2]Center for Cancer Research, National Cancer Institute, NIH, Bethesda, MA 20892 USA

[3]Department of Molecular Cardiology, Lerner Research Institute, Cleveland Clinic, Cleveland, OH 44195 USA

[4]Laboratory of Fluorescence Dynamics and Department of Biomedical Engineering, University of California Irvine, Irvine, CA 92697 USA

Summary

Background—A complex network of putative molecular interactions underlies the architecture and function of cell-matrix adhesions. Most of these interactions are implicated from co-immunoprecipitation studies using expressed components; but few have been demonstrated or characterized functionally in living cells.

Results—We introduce fluorescence fluctuation methods to determine, at high spatial and temporal resolution, ‘when’ and ‘where’ molecular complexes form and their stoichiometry in nascent adhesions (NAs). We focus on integrin-associated molecules implicated in integrin-activation and in the integrin-actin linkage in NAs and show that these molecules form integrin containing complexes hierarchically within the adhesion itself. Integrin and kindlin reside in a molecular complex as soon as adhesions are visible; talin, while also present early, associates with the integrin-kindlin complex only after NAs have formed and in response to myosin II activity. Furthermore, talin and vinculin association precedes the formation of the integrin-talin complex. Finally, α-actinin enters NAs periodically and in clusters that transiently associate with integrins. The absolute number and stoichiometry of these molecules varies among the molecules studied and changes as adhesions mature.

Conclusions—These observations suggest a working model for NA assembly, whereby transient α-actinin- integrin complexes help nucleate NAs within the lamellipodium. Subsequently integrin complexes containing kindlin, but not talin, emerge. Once NAs have formed, myosin II

*Corresponding author (ab8su@virginia.edu).

activity promotes talin association with the integrin-kindlin complex in a stoichiometry consistent with each talin molecule linking two integrin-kindlin complexes.

Introduction

Cell-matrix adhesion is central to many modes of cell migration, a process involved in pathologies such as cancer, atherosclerosis, and chronic inflammatory diseases [1]. Adhesions are comprised of networks of molecular interactions [2] and generate traction and signals that mediate and regulate migration [3]. Integrin receptors are central components of this network [4]. They bind several different extracellular matrix ligands, organize signaling complexes, and connect to the actin cytoskeleton through interactions with a large number of different molecules that bind to them either directly or indirectly [2, 5]. Despite a plethora of information on the *in vitro* binding interactions among integrin-and adhesion-associated molecules, 'where' and 'when' these interactions occur determines adhesion and cellular function and remains largely unknown.

Talin and kindlin bind integrin directly and regulate both its activation and the formation of adhesions [6]. Talin1 knockdown shows diminished activation of $\alpha_{IIb}\beta_3$, $\alpha_v\beta_3$, and $\alpha_5\beta_1$ integrins [7] and impaired adhesion formation [8]. Kindlins, more recently identified as adhesion components [9], are also required for talin-mediated integrin activation [10]. Kindlin-3 deficient platelets, for example, fail to activate integrins despite normal talin expression [11]. While the overlapping functions of these two molecules are clear, 'when' and 'where' talin and kindlin cooperate to activate integrins during adhesion formation is not known. Current models suggest either simultaneous or sequential binding of both molecules to the cytoplasmic tail of the β integrin subunit [12].

A similar conundrum exists for the interactions between integrin and its associated actin-binding adhesion partners. Talin, vinculin, and α-actinin are all thought to be part of a linkage, between integrin and the actin cytoskeleton, that is required for traction and adhesion formation [13, 14]. Both talin and α-actinin bind integrin and actin directly [15, 16]. Vinculin binds talin and activates it; it also binds to actin and α-actinin [17, 18], and like α-actinin and talin, serves to link integrins to actin filaments and indirectly, cluster integrins [18, 19]. Thus, even with this small set of molecules, there are many potential interactions that mediate the linkages from integrin to actin. It seems unlikely that all exist simultaneously; but how all of these potential interactions occur and the adhesion types in which they reside is also not known. Further, it is unclear whether these molecules are recruited independently or reside as preformed, pre-activated cytoplasmic complexes.

These are only a few of the ~200 molecules thought to associate with adhesions [2]. Their interactions have been inferred largely from immunoprecipitations using purified, endogenous or overexpressed components. To date, few studies have addressed their existence and function in living cells [14, 20–23]. Recent developments in fluorescence fluctuation methods provide a toolbox for addressing these kinds of molecular interactions [20, 24, 25]. The methods rely on the analysis of molecular intensity fluctuations from fluorescently tagged adhesion molecules and provide measurements of dynamics, concentrations, and aggregation states. When implemented in a dual-color mode, co-

fluctuations in fluorescence intensity reveal the presence and composition of molecular complexes.

In this study, we introduce fluorescence fluctuation methods to determine; at high spatial and temporal resolution the formation and stoichiometry of molecular complexes in the nascent adhesions that populate protrusions in migrating CHO cells. We focus on kindlin, talin, vinculin, and α-actinin – integrin-associated molecules implicated in integrin activation or cross-linking to the actin cytoskeleton. We show that whereas these molecules are recruited at the same time to adhesions, their interactions emerge hierarchically within the adhesion itself instead of entering as performed complexes from the neighboring cell membrane or cytoplasm. $\alpha_5\beta_1$ integrin and kindlin2 are detected in a molecular complex at the onset of nascent adhesion formation; however, talin1 associates with $\alpha_5\beta_1$ integrin and kindlin2 only after nascent adhesions have formed and in response to myosin II activity. In contrast, talin1 and vinculin are present in a complex as the nascent adhesions assemble. Furthermore, α-actinin enters adhesions in periodic clusters that associate transiently with integrins. We also show that the stoichiometries underlying these interactions vary as adhesions mature. Whereas $\alpha_5\beta_1$ integrin and kindlin2 are present in a 1:1 ratio in nascent adhesions, talin is present in a 0.5:1 ratio with integrin. However, as adhesions mature, talin1 increases to a 1:1 ratio with $\alpha_5\beta_1$ integrin and kindlin2. Together, these results point to a hierarchical formation of molecular interactions during nascent adhesion formation.

Results

$\alpha_5\beta_1$ integrin and kindlin2 associate in a molecular complex as adhesions assemble

To determine whether talin and kindlin reside in nascent adhesions, we co-expressed mCherry-paxillin, an early marker of nascent adhesions [26], with mGFP tagged talin1, kindlin2, or the α_5 integrin subunit in CHOK1 cells. $\alpha_5\beta_1$ integrin, talin1, and kindlin2 all localize to nascent adhesions (Figure 1A, arrowheads) and enter at about the same time, but with differing assembly rates (Figure 1B). Whereas $\alpha_5\beta_1$ integrin and kindlin2 enter with indistinguishable kinetics, talin1 entered slightly faster. These data suggest that the entry of talin is uncoupled from that of either $\alpha_5\beta_1$ integrin or kindlin2, and raises the possibility that the latter two may enter as a preformed complex.

To determine whether the similar assembly rates for $\alpha_5\beta_1$ integrin and kindlin2 in nascent adhesions are due to molecular associations that form before or as adhesions assemble, we used cross-variance analysis [24]. This method detects the presence of molecular complexes using co-variance analysis of fluorescence fluctuations arising from the dynamic exchange of molecular complexes in adhesions. Molecules that are unassociated will enter and leave adhesions independently and show no cross-variance (B_{cc}); however molecules that reside in a common complex will enter and leave together and show a positive cross-variance.

We calculated temporal maps of (B_{cc}); using image time series of CHOK1 cells expressing α_5 integrin-mGFP and mCherry-kindlin2 (Figure 1C). Figure 1D is a representative plot of the fluorescence intensity of $\alpha_5\beta_1$ integrin and kindlin2 in a nascent adhesion and the corresponding (B_{cc}) values calculated from different stages of adhesion formation. We observed positive (B_{cc}) values as the adhesions start to assemble, and they persisted after the

adhesions formed. We observed a similar positive (B_{cc}) value for the positive controls, mGFP-talin1-mCherry and mCherry-paxillin-mGFP, throughout nascent adhesion formation (Figure S2). In contrast, the (B_{cc}) values measured in pixels before the adhesions were visible and from a negative control consisting of two non-interacting molecules, GAP-mGFP and GAP-mCherry, showed minimal cross-variance (Figure 1E). Furthermore, cells expressing $\alpha_5\beta_1$ integrin and a kindlin2 mutant (Q614A/W615A) that lacks integrin binding activity [27] show neither specific localization to adhesions nor positive cross-variance (Figure S1). These data suggest that $\alpha_5\beta_1$ integrin and kindlin2 reside in a common complex as adhesions form and stabilize (Figure 1E). We also observed lower (B_{cc}) values during disassembly and post-disassembly, suggesting that some adhesion molecules dissociate from disassembling adhesions independently rather than in complexes.

To determine whether $\alpha_5\beta_1$ integrin and kindlin2 are pre-associated before adhesions form, we compared the (B_{cc}) values in adhesions with areas outside adhesions, i.e., between nascent adhesions (e.g., Area 1–3) and farther away (e.g., Area 4–6) from the adhesion rich protrusive edge (Figure 1C &E). In both of these areas, the (B_{cc}) values were calculated from more than fifteen areas in each region. Even though the results were statistically different from those seen in the negative controls and the preassembly pixels in regions where adhesions emerge, they were statistically different from the (B_{cc}) values calculated from the assembly and stability phases showing that $\alpha_5\beta_1$ integrin and kindlin2 are most likely not associated in a complex at those locations. Taken together, the data suggest that $\alpha_5\beta_1$ integrin and kindlin2 do not interact in the plasma membrane outside adhesions; but rather, they assemble into a complex as they enter the adhesion itself.

Talin associates with $\alpha_5\beta_1$ integrin and kindlin2 after nascent adhesions assemble and in response to myosin II activation

We next determined whether talin1 associates with $\alpha_5\beta_1$ integrin in adhesions, using cross-variance analysis on CHOK1 cells expressing α_5 integrin-mGFP and mCherry-talin1. The (B_{cc}) values were near control values as the adhesions assembled but then showed positive cross-variance once the nascent adhesions formed (Figure 2A). This contrasts kindlin2 and $\alpha_5\beta_1$ integrin, which reside in a complex as nascent adhesions assemble. A talin1 mutant (R358A) that does not bind integrins showed weaker localization, more diffuse expression, and no detectable cross-variance (Figure S1) [28].

Next, we investigated associations between talin1 and kindlin2, using mGFP-talin1 and mCherry-kindlin2. Like talin1 and $\alpha_5\beta_1$ integrin, they did not show statistically significant cross-variance values as nascent adhesions assembled but did show positive (B_{cc}) values once the nascent adhesions assembled (Figure 2B). This reveals that mGFP-talin1 and mCherry-kindlin2 do not reside in a common complex until nascent adhesions have assembled, as observed for talin1 and $\alpha_5\beta_1$ integrin. Taken together, these observations show that whereas talin1, kindlin2, and $\alpha_5\beta_1$ integrin all enter nascent adhesions as they begin to form, kindlin2 and $\alpha_5\beta_1$ integrin associate in a complex early, during the assembly process, and talin enters the complex after the adhesions have assembled.

Since we observed a delayed association between talin1 and $\alpha_5\beta_1$ integrin in adhesions, we next asked whether it reflects the myosin dependent maturation into focal complexes and

focal adhesions [26]. To distinguish between these, we inhibited myosin II activation using Y27632, an inhibitor of ROCK activity and adhesion maturation [29]. When we treated U2OS cells expressing α_5 integrin-mGFP and talin-mCherry with 30 μM Y27632, nascent adhesions formed but did not mature into elongated adhesions (Figure 2C). mCherry-talin1 localized in these nascent adhesions (Figure 2D); however, it did not show detectable (B_{cc}) values with α_5 integrin-mGFP, even at time periods well beyond those when complexes are detected in control cells (Figure 2E). In contrast, kindlin2 showed positive cross-variance with $\alpha_5\beta_1$ integrin in nascent adhesions, even after ROCK inhibition, as it did in untreated controls (Figure 2F). These data suggest that $\alpha_5\beta_1$ integrin-kindlin2 interactions are independent of ROCK mediated myosin II activation; whereas $\alpha_5\beta_1$ integrin-talin1 interactions require it, demonstrating a possible role for myosin II activity in the formation of a stable talin-integrin complex. These observations agree with studies showing that force coupling mediated through local depletion of PtdIns(4,5)P2 regulates talin but not kindlin recruitment to adhesions [30].

Talin and vinculin reside in a molecular complex as adhesions assemble and mature

Since vinculin is implicated in talin activation and incorporation into adhesions [18, 31], we used cross-variance analysis to determine when they associate in nascent adhesions. In cells expressing vinculin-mGFP and mCherry-talin1 (Figure 3A), positive cross-variance between talin1 and vinculin appeared at the onset of nascent adhesion formation (Figure 3A and 3B) and persisted even after the adhesions formed and elongated (Figure 3B). These data suggest that talin1 and vinculin reside in a complex as nascent adhesions form and mature. Interestingly, positive (B_{cc}) were predominant at the end, proximal to the protrusion of the elongated adhesions, suggesting a preferential, localized recruitment of the complex (Figure 3C). Furthermore, faster sampling was required to capture the exchange of talin and vinculin as a complex when compared to the sampling time for talin1 and $\alpha_5\beta_1$ integrin, showing that they exchange independently of integrin (Figure S2). This association is not apparent in the cytoplasm using ccRICS (Figure S3), but emerges in adhesions where force-mediated vinculin activation, required for talin binding [32, 33] is thought to occur [34].

α-Actinin displays a distinct pattern of entry and complex formation in nascent adhesions

α-Actinin binds β_1 integrin in vitro and is thought to be part of the integrin-actin linkage [15]. To determine ‘if’ and ‘when’ α-actinin and integrin associate in a complex, we studied their relative rates of entry in nascent adhesions using CHOK1 cells expressing α_5 integrin-mGFP and α-actinin-mCherry (Figure 4A). α-actinin entered nascent adhesions at a rate faster than that of $\alpha_5\beta_1$ integrin (Figure 4B). Its intensity increased in periodic spikes (Figure 4A), with an average period of approximately 20 seconds, suggesting it enters adhesions in discrete clusters. We often also observed small intensity increases for α_5 integrin coincident with the α-actinin spikes, suggesting that they may be associated. The cross-variance analysis revealed positive (B_{cc}) values for α-actinin and $\alpha_5\beta_1$ integrin only during the periodic α-actinin intensity spikes, showing that indeed the molecules transiently associate at discrete, relatively short times during nascent adhesion assembly (Figure 4C).

This contrasts talin1, which forms molecular complexes with $\alpha_5\beta_1$ integrin only after nascent adhesions have formed. We then asked whether the delayed association between

integrin and talin1 during nascent adhesion formation is due to α-actinin binding [35]. To do this, we measured the onset of molecular complex formation between integrin and talin1 in CHOK1 cells with α-actinin knocked down. Interestingly, talin1 overexpression rescues the inhibition of adhesion and protrusion in the α-actinin knockdowns [26] (Figure 4D) and therefore is able to substitute for it during adhesion formation. Furthermore, talin is now present with integrin in molecular complexes as nascent adhesions form (Figure 4E). Thus, in the absence of α-actinin, talin associates with $\alpha_5\beta_1$ integrin, which is the only integrin present in CHOK1 cells, to rescue the formation and turnover of nascent adhesions.

$\alpha_5\beta_1$ integrin displays differing stoichiometry relative to its binding partners

Since integrin actin-binding partners possess multiple binding sites as well as dimerization domains, which could serve to cross-link them to each other as well as to integrins [6, 31, 36], we estimated the number of molecules and stoichiometry of these molecules using fluctuation methods (see supplemental information, Figures S4 & S5). By comparing the nascent adhesion intensities to the intensity of a known monomer (GAP-mGFP), we estimated there are ~ 6.5 ± 1.3 $\alpha_5\beta_1$ integrins in a nascent adhesion; this is ~ two fold higher than that in pixels adjacent to the nascent adhesions (Figure 5A). These $\alpha_5\beta_1$ integrins also reside in adhesions in aggregates with an average of ~ 6 ± 1 molecules, and in off adhesion regions with an average aggregate of ~ 2 ± 1 molecules (Figure 5B). Our off-adhesion results are consistent with previous measurements of integrin membrane numbers [25] as well as fibronectin-integrin binding studies showing that fibronectin trimers are sufficient for binding to the actin cytoskeleton [37].

We next determined the effect of integrin expression level and matrix density on the numbers of integrins in adhesions. In low expressing cells, fewer adhesions formed, and for those that did form, the number of molecules was similar to that seen in off-adhesion regions (Figure 5A). In contrast, the fibronectin density did not affect the number of integrin molecules in adhesions within the 5-fold range that promoted adhesion (Figure 5C). This suggests that the number of integrin molecules in nascent adhesions is primarily dictated by intrinsic factors rather than fibronectin density.

We then compared the relative numbers of kindlin2, talin1, and vinculin to $\alpha_5\beta_1$ integrin. Whereas the numbers of kindlin2 and integrin were similar (1:1), the number of talin1 molecules was ~1/2 that of $\alpha_5\beta_1$ integrin, values that are also supported by variance of the integrin-talin-kindlin complex. Vinculin displayed ~ 1.3 times the number of integrin molecules in the nascent adhesions; the variability was much greater when compared to kindlin2, talin1, and $\alpha_5\beta_1$ integrin, with more adhesions exhibiting a higher number of molecules (Figure 5D). α-actinin numbers in individual nascent adhesions was the largest among all molecules. The number of molecules in each α-actinin intensity spike contained 3–4 molecules reaching a plateau of 14 molecules/nascent adhesion (Figure 5E). Furthermore, for mature elongated focal adhesions, we observed a linear increase in all adhesion molecules as the size of the adhesion increased (Figure 5F). The relative vinculin density was the highest (4x the other molecules); whereas, the stoichiometry between kindlin2, talin1, and $\alpha_5\beta_1$ integrin was 1:1, in agreement with previous data [14].

Discussion

A complex network of molecular interactions underlies the signaling activities and ECM-actin linkage of cell adhesions [2]; and is particularly apparent in an integrated cellular process like migration [5]. Despite the plethora of biochemical information identifying potential interactions among the molecules in cell adhesions, their location, dynamics, stoichiometry, and regulation are largely unknown. To date, the absence methods that capture molecular associations and numbers robustly with high spatial and temporal resolution have challenged their measurement.

In this study, we identify integrin complexes that contain integrin-activating molecules, like kindlin and talin, and actin-linking molecules, like talin, vinculin, and α-actinin, during the formation of nascent adhesions. We also measure the number of these molecules in the adhesions. We do this by extending and optimizing newly developed fluorescence fluctuation methods, which can produce high spatial and temporal resolution maps of protein complexes [20, 24]. We find that all of the molecules studied enter nascent adhesions as they first become visible; however their rate of addition, absolute numbers, and incorporation into molecular complexes in adhesions differs. For example, integrin–kindlin and talin–vinculin are present in complexes as soon as they appear in adhesions; whereas talin-integrin and kindlin-talin reside in common molecular complexes only after the adhesion has formed. In contrast, α-actinin enters at the fastest rate and in spikes that form transient associations with integrin.

The differential molecular associations between integrin and two of its binding partners, kindlin and talin, in adhesions bears on their role in integrin function. Considerable in vitro and in vivo evidence suggests that integrin activation requires the binding of both kindlin and talin [7, 10]. Our cross-variance data suggest that this occurs after nascent adhesions have already formed and not in regions adjacent to the adhesions. Therefore, $\alpha_5\beta_1$ integrin is likely not pre-activated before nascent adhesions have formed, which is not consonant with observations that integrin is pre-activated at the leading edge [38, 39]. This could be due to the different integrin studied ($\alpha_v\beta_3$ vs $\alpha_5\beta_1$) or to the lower resolution that did not resolve nascent adhesions. Our data also does not support a model in which the binding of $\alpha_5\beta_1$ integrin to talin directly nucleates nascent adhesions, as they do not appear to reside in a complex until after the nascent adhesion has formed. Since talin is present in nascent adhesions, as soon as they are visible, its interaction with some other molecule(s), like vinculin, RIAM [40, 41] or FAK [42] likely recruits it to adhesions. Finally, the talin-kindlin-integrin complex and therefore integrin activation requires myosin II, presumably through cross-linking and force generation activities [43].

Our observations extend previous studies. Talin-null cells have only small adhesions that adhere weakly and do not mature. Thus, adhesions can form without talin; but they are unable to support or respond to the subsequent force that drives their maturation [8]. This is supported by recent findings that suggest that integrin binding to fibronectin [44] and recruitment to adhesions is independent of talin [22], possibly due to competitive binding with α-actinin [35]. Our data also support suggestions that kindlin and talin associate with integrins sequentially [45, 46] with kindlin associating first and then talin [12]. The initial

binding of kindlin might be required to facilitate talin integrin binding via displacement of integrin inhibitors such as filamin from the β integrin cytoplasmic tail [47] and recruitment of ILK [48] and migfilin [9, 49]. Previous observations also show that nascent adhesions can form without myosin II activity; whereas myosin cross-linking and force are required for their subsequent adhesion maturation [26, 50]. Our studies show that talin-integrin complex is myosin II sensitive, which is consistent with studies showing that integrin, talin as well as vinculin are all thought to undergo force induced conformation changes and/or sense force in adhesions [30, 34, 51, 52]. Force in adhesions also stabilizes integrin-fibronectin binding interactions [52].

So, what interactions nucleate adhesions and their subsequent maturation? The number and cluster analyses provide insights. The clustering of integrins is thought to be an early event [53–55]. Since kindlin is monomeric with a single integrin binding site and present in a 1:1 ratio with integrin in nascent adhesions, it is unlikely that it directly mediates the initial clustering of integrins. However, its association with other binding partners like ILK and migfilin could indirectly induce clustering [48, 49, 56]. α-actinin, another candidate, is a homodimer, binds actin, and is present throughout the lamellipodium in a high stoichiometry with respect to integrin in adhesions. However, if it does nucleate adhesions, it does so only transiently and through large clusters. Once adhesions begin to mature, talin could be a primary link to actin and mediate integrin clustering; since its ratio to integrin is 1:2, suggesting that it either crosslinks through the two integrin binding sites at its N-terminal head and C-terminal tail domains [16] or through its binding to vinculin, which binds to α-actinin.

In summary, the integrin binding and actin linkage molecules that we have studied are all present in nascent adhesions as soon as they are visible and persist as they mature; however, the molecular interactions and stoichiometry change, reflecting an internal reorganization as the adhesion forms and matures. It is still not clear which molecular interactions drive adhesion formation. Some models propose that integrins pre-bound to activating partners at the cell edge and probe the ECM for adhesion sites [38, 39]. Other studies show that adhesion formation is driven by actin polymerization and organization [26]. While kindlin and α-actinin remain viable candidates for nucleating adhesion formation through their early association with integrin, the dimeric nature of α-actinin and its transient association with $\alpha_5\beta_1$ integrin makes it an attractive potential nucleator. The large α-actinin clusters that associate transiently with integrin contain the same number of molecules (3) as that for the off-adhesion integrin clusters, suggesting that α-actinin may facilitate an initial binding step of integrin clusters to the actin cytoskeleton, which is then replaced by a longer-lived interaction, and then ultimately by talin [35]. Whatever model emerges, however, it will now be informed by our observation that an important class of integrin interactions occurs transiently and hierarchically within the adhesion.

Experimental Procedures

Nascent Adhesion Analysis

The nascent adhesions were manually selected in protruding regions and the corresponding pixel locations inputted in Matlab 7.7.0 (The Mathworks, Natick, MA). The fluorescence

intensity time traces for individual adhesions were measured by spatially averaging a 3 by 3 pixel region centered at the adhesion pixel location for each image in the time series. Background intensity was corrected for by subtracting from an image series an average intensity value corresponding to background regions away from the cell. Fluorescence bleaching was estimated using the intensity decay of focal adhesions over the time course of image series acquisition. It was then accounted for by adding to each image in the image series the percent of intensity lost at that given time point. Adhesion assembly rates were estimated from 30–40 adhesions in 6–8 cells following [26]. In the number of molecules measurements, the intensities of individual adhesions were integrated over a 3 by 3 pixel region for nascent adhesions and over the entire pixel location of larger focal adhesions. For α-actinin number measurements in nascent adhesions, we subtracted an average intensity corresponding to lamellipodial regions where no adhesions are visible. To yield the total number of molecules, the intensity values of the adhesions were normalized by the molecular fluorescence of mGFP (for more information, see supplemental data and methods).

Fluorescence variance and cross-variance analysis

We used fluorescence variance analysis also known as number and brightness (N&B) to determine the aggregation states and molecular interactions (cross-N&B) in adhesions [24]. Using SimFCS software (Laboratory of Fluorescence Dynamics, University of California, Irvine, CA), we calculated the apparent brightness B and cross-brightness (B_{cc}) parameters from single or dual-channel image time series. The apparent brightness B(i,j) parameter, for a given pixel location (x_i, x_j) in a single channel image time series is defined as:

$$B(x_i, y_j) = \frac{1}{s} \cdot \frac{\sigma^2_{i,j} - \sigma^2_0}{\langle I(x_{i,}y_j)\rangle_t - \text{offset}} = \varepsilon + 1 \quad (1)$$

$\langle I(x_i, x_j)\rangle_t$ and $\sigma^2_{i,j}$ are the pixel average intensity and variance over time (*t*) respectively; ε is the intrinsic molecular brightness, which reflects the total number of emitting molecules in a complex and can vary depending on the image acquisition settings that affect fluorescence excitation and detection.

The offset parameter and readout noise σ^2_0 were determined from the distribution of the digital counts of a background region in the image time series. The *S* factor was set to a value that yields a background brightness value of 1(B/S=1). Contributions from slow fluctuations due to photobleaching and mechanical drift effects were corrected for using a moving average filter (~ 20–25 seconds). The aggregation state of adhesion molecules was determined by calibration of the measured apparent brightness parameter relative to that measured from the membrane targeting sequence of mGFP tagged GAP43 [20].

$$\text{Degree of Aggregation} = \frac{B_{Adh} - 1}{B_{GAP} - 1} \quad (2)$$

For detecting molecular interactions in adhesions, we calculate the cross-variance (B_{cc}) parameter at a given pixel location (x_i, x_j) as:

$$B_{cc}(x_i, y_j) = \frac{\sigma(x_i, y_j)^2_{cc}}{\sqrt{\langle I_1(x_i, y_j)\rangle_t \langle I_2(x_i, y_j)\rangle_t}} \quad (3)$$

$\langle I_1(x_i, x_j)\rangle_t$ and $\langle I_2(x_i, x_j)\rangle_t$ are the fluorescence average intensity for channels 1 and 2. $\sigma(x_i, y_j)^2_{cc}$ is the fluorescence intensity cross-variance between channels 1 and 2 for time, t, and is defined as:

$$\sigma(x_i, y_j)^2_{cc} = \frac{1}{t} \cdot \sum_t (I_1(x_i, y_j, t) - \langle I_1(x_i, y_j)\rangle_t).(I_2(x_i, y_j, t) - \langle I_2(x_i, y_j)\rangle_t) \quad (4)$$

I_1 (x_i, y_i, t) and I_2 (x_i, y_i, t) are the fluorescence pixel intensity at time, t, for channels 1 and 2 respectively.

If molecules represented by fluorescence intensity in two channels (wavelengths), channel 1 and 2, are non-interacting, their fluorescence fluctuations will be independent and the cross-variance will be centered around zero. In contrast, interacting species will produce positive (B_{cc}) values. As the negative control, GAP-mGFP and GAP-mCherry, which localize independently to the cell membrane, are not known to interact and therefore do not display positive cross-variance values 20]. As a positive control, we used mCherry-paxillin-mGFP; an adhesion marker tagged with two fluorescent probes and therefore produces correlated movement and positive cross-variance.

Supplementary Material

Refer to Web version on PubMed Central for supplementary material.

Acknowledgments

We thank D. Critchley for helpful comments and discussion. This research was supported by NIH grants (R01 GM023244) and the Cell Migration Consortium (U54 GM064346) for A.R. Horwitz and by NIH grants, NIH P41-GM103540 and NIH P50-GM076516, for E. Gratton.

References

1. Friedl P, Gilmour D. Collective cell migration in morphogenesis, regeneration and cancer. Nat Rev Mol Cell Biol. 2009; 10:445–457. [PubMed: 19546857]
2. Zaidel-Bar R, Itzkovitz S, Ma'ayan A, Iyengar R, Geiger B. Functional atlas of the integrin adhesome. Nat Cell Biol. 2007; 9:858–867. [PubMed: 17671451]
3. Parsons JT, Horwitz AR, Schwartz MA. Cell adhesion: integrating cytoskeletal dynamics and cellular tension. Nat Rev Mol Cell Biol. 2010; 11:633–643. [PubMed: 20729930]
4. Hynes RO. Integrins: bidirectional, allosteric signaling machines. Cell. 2002; 110:673–687. [PubMed: 12297042]
5. Vicente-Manzanares M, Choi CK, Horwitz AR. Integrins in cell migration--the actin connection. J Cell Sci. 2009; 122:199–206. [PubMed: 19118212]
6. Calderwood DA, Campbell ID, Critchley DR. Talins and kindlins: partners in integrin-mediated adhesion. Nat Rev Mol Cell Biol. 2013; 14:503–517. [PubMed: 23860236]
7. Tadokoro S, Shattil SJ, Eto K, Tai V, Liddington RC, de Pereda JM, Ginsberg MH, Calderwood DA. Talin binding to integrin beta tails: a final common step in integrin activation. Science. 2003; 302:103–106. [PubMed: 14526080]

8. Zhang X, Jiang G, Cai Y, Monkley SJ, Critchley DR, Sheetz MP. Talin depletion reveals independence of initial cell spreading from integrin activation and traction. Nat Cell Biol. 2008; 10:1062–1068. [PubMed: 19160486]
9. Tu Y, Wu S, Shi X, Chen K, Wu C. Migfilin and Mig-2 link focal adhesions to filamin and the actin cytoskeleton and function in cell shape modulation. Cell. 2003; 113:37–47. [PubMed: 12679033]
10. Ma YQ, Qin J, Wu C, Plow EF. Kindlin-2 (Mig-2): a co-activator of beta3 integrins. J Cell Biol. 2008; 181:439–446. [PubMed: 18458155]
11. Moser M, Nieswandt B, Ussar S, Pozgajova M, Fassler R. Kindlin-3 is essential for integrin activation and platelet aggregation. Nat Med. 2008; 14:325–330. [PubMed: 18278053]
12. Moser M, Legate KR, Zent R, Fassler R. The tail of integrins, talin, and kindlins. Science. 2009; 324:895–899. [PubMed: 19443776]
13. Calderwood DA, Shattil SJ, Ginsberg MH. Integrins and actin filaments: reciprocal regulation of cell adhesion and signaling. J Biol Chem. 2000; 275:22607–22610. [PubMed: 10801899]
14. Kanchanawong P, Shtengel G, Pasapera AM, Ramko EB, Davidson MW, Hess HF, Waterman CM. Nanoscale architecture of integrin-based cell adhesions. Nature. 2010; 468:580–584. [PubMed: 21107430]
15. Otey CA, Pavalko FM, Burridge K. An interaction between alpha-actinin and the beta 1 integrin subunit in vitro. J Cell Biol. 1990; 111:721–729. [PubMed: 2116421]
16. Critchley DR. Biochemical and structural properties of the integrin-associated cytoskeletal protein talin. Annu Rev Biophys. 2009; 38:235–254. [PubMed: 19416068]
17. Bois PR, Borgon RA, Vonrhein C, Izard T. Structural dynamics of alpha-actinin-vinculin interactions. Mol Cell Biol. 2005; 25:6112–6122. [PubMed: 15988023]
18. Humphries JD, Wang P, Streuli C, Geiger B, Humphries MJ, Ballestrem C. Vinculin controls focal adhesion formation by direct interactions with talin and actin. J Cell Biol. 2007; 179:1043–1057. [PubMed: 18056416]
19. Shen K, Tolbert CE, Guilluy C, Swaminathan VS, Berginski ME, Burridge K, Superfine R, Campbell SL. The vinculin C-terminal hairpin mediates F- actin bundle formation, focal adhesion, and cell mechanical properties. J Biol Chem. 2011; 286:45103–45115. [PubMed: 22052910]
20. Choi CK, Zareno J, Digman MA, Gratton E, Horwitz AR. Cross-correlated fluctuation analysis reveals phosphorylation-regulated paxillin-FAK complexes in nascent adhesions. Biophys J. 2011; 100:583–592. [PubMed: 21281572]
21. Patla I, Volberg T, Elad N, Hirschfeld-Warneken V, Grashoff C, Fassler R, Spatz JP, Geiger B, Medalia O. Dissecting the molecular architecture of integrin adhesion sites by cryo-electron tomography. Nat Cell Biol. 2010; 12:909–915. [PubMed: 20694000]
22. Rossier O, Octeau V, Sibarita JB, Leduc C, Tessier B, Nair D, Gatterdam V, Destaing O, Albiges-Rizo C, Tampe R, Cognet L, Choquet D, Lounis B, Giannone G. Integrins beta1 and beta3 exhibit distinct dynamic nanoscale organizations inside focal adhesions. Nat Cell Biol. 2012; 14:1057–1067. [PubMed: 23023225]
23. Zamir E, Geiger B, Kam Z. Quantitative multicolor compositional imaging resolves molecular domains in cell-matrix adhesions. PLoS One. 2008; 3:e1901. [PubMed: 18382676]
24. Digman MA, Wiseman PW, Choi C, Horwitz AR, Gratton E. Stoichiometry of molecular complexes at adhesions in living cells. Proc Natl Acad Sci U S A. 2009; 106:2170–2175. [PubMed: 19168634]
25. Wiseman PW, Brown CM, Webb DJ, Hebert B, Johnson NL, Squier JA, Ellisman MH, Horwitz AF. Spatial mapping of integrin interactions and dynamics during cell migration by image correlation microscopy. J Cell Sci. 2004; 117:5521–5534. [PubMed: 15479718]
26. Choi CK, Vicente-Manzanares M, Zareno J, Whitmore LA, Mogilner A, Horwitz AR. Actin and alpha-actinin orchestrate the assembly and maturation of nascent adhesions in a myosin II motor-independent manner. Nat Cell Biol. 2008; 10:1039–1050. [PubMed: 19160484]
27. Shi X, Ma YQ, Tu Y, Chen K, Wu S, Fukuda K, Qin J, Plow EF, Wu C. The MIG-2/integrin interaction strengthens cell-matrix adhesion and modulates cell motility. J Biol Chem. 2007; 282:20455–20466. [PubMed: 17513299]

28. Garcia-Alvarez B, de Pereda JM, Calderwood DA, Ulmer TS, Critchley D, Campbell ID, Ginsberg MH, Liddington RC. Structural determinants of integrin recognition by talin. Mol Cell. 2003; 11:49–58. [PubMed: 12535520]
29. Narumiya S, Ishizaki T, Uehata M. Use and properties of ROCK-specific inhibitor Y-27632. Methods Enzymol. 2000; 325:273–284. [PubMed: 11036610]
30. Legate KR, Takahashi S, Bonakdar N, Fabry B, Boettiger D, Zent R, Fassler R. Integrin adhesion and force coupling are independently regulated by localized PtdIns(4,5)2 synthesis. Embo J. 2011; 30:4539–4553. [PubMed: 21926969]
31. Carisey A, Ballestrem C. Vinculin, an adapter protein in control of cell adhesion signalling. Eur J Cell Biol. 2011; 90:157–163. [PubMed: 20655620]
32. Cohen DM, Kutscher B, Chen H, Murphy DB, Craig SW. A conformational switch in vinculin drives formation and dynamics of a talin-vinculin complex at focal adhesions. J Biol Chem. 2006; 281:16006–16015. [PubMed: 16608855]
33. Chen H, Choudhury DM, Craig SW. Coincidence of actin filaments and talin is required to activate vinculin. J Biol Chem. 2006; 281:40389–40398. [PubMed: 17074767]
34. Carisey A, Tsang R, Greiner AM, Nijenhuis N, Heath N, Nazgiewicz A, Kemkemer R, Derby B, Spatz J, Ballestrem C. Vinculin regulates the recruitment and release of core focal adhesion proteins in a force-dependent manner. Curr Biol. 2013; 23:271–281. [PubMed: 23375895]
35. Roca-Cusachs P, del Rio A, Puklin-Faucher E, Gauthier NC, Biais N, Sheetz MP. Integrin-dependent force transmission to the extracellular matrix by alpha-actinin triggers adhesion maturation. Proc Natl Acad Sci U S A. 2013; 110:E1361–1370. [PubMed: 23515331]
36. Otey CA, Carpen O. Alpha-actinin revisited: a fresh look at an old player. Cell Motil Cytoskeleton. 2004; 58:104–111. [PubMed: 15083532]
37. Coussen F, Choquet D, Sheetz MP, Erickson HP. Trimers of the fibronectin cell adhesion domain localize to actin filament bundles and undergo rearward translocation. J Cell Sci. 2002; 115:2581–2590. [PubMed: 12045228]
38. Kiosses WB, Shattil SJ, Pampori N, Schwartz MA. Rac recruits high-affinity integrin alphavbeta3 to lamellipodia in endothelial cell migration. Nat Cell Biol. 2001; 3:316–320. [PubMed: 11231584]
39. Galbraith CG, Yamada KM, Galbraith JA. Polymerizing actin fibers position integrins primed to probe for adhesion sites. Science. 2007; 315:992–995. [PubMed: 17303755]
40. Lee HS, Anekal P, Lim CJ, Liu CC, Ginsberg MH. Two modes of integrin activation form a binary molecular switch in adhesion maturation. Mol Biol Cell. 2013; 24:1354–1362. [PubMed: 23468527]
41. Goult BT, Zacharchenko T, Bate N, Tsang R, Hey F, Gingras AR, Elliott PR, Roberts GC, Ballestrem C, Critchley DR, Barsukov IL. RIAM and vinculin binding to talin are mutually exclusive and regulate adhesion assembly and turnover. J Biol Chem. 2013; 288:8238–8249. [PubMed: 23389036]
42. Lawson C, Lim ST, Uryu S, Chen XL, Calderwood DA, Schlaepfer DD. FAK promotes recruitment of talin to nascent adhesions to control cell motility. J Cell Biol. 2012; 196:223–232. [PubMed: 22270917]
43. Vicente-Manzanares M, Ma X, Adelstein RS, Horwitz AR. Non-muscle myosin II takes centre stage in cell adhesion and migration. Nat Rev Mol Cell Biol. 2009; 10:778–790. [PubMed: 19851336]
44. Roca-Cusachs P, Gauthier NC, Del Rio A, Sheetz MP. Clustering of alpha(5)beta(1) integrins determines adhesion strength whereas alpha(v)beta(3) and talin enable mechanotransduction. Proc Natl Acad Sci U S A. 2009; 106:16245–16250. [PubMed: 19805288]
45. Bledzka K, Liu J, Xu Z, Perera HD, Yadav SP, Bialkowska K, Qin J, Ma YQ, Plow EF. Spatial coordination of kindling-2 with talin head domain in interaction with integrin beta cytoplasmic tails. J Biol Chem. 2012; 287:24585–24594. [PubMed: 22648415]
46. Kim C, Ye F, Ginsberg MH. Regulation of integrin activation. Annu Rev Cell Dev Biol. 2011; 27:321–345. [PubMed: 21663444]

47. Kiema T, Lad Y, Jiang P, Oxley CL, Baldassarre M, Wegener KL, Campbell ID, Ylanne J, Calderwood DA. The molecular basis of filamin binding to integrins and competition with talin. Mol Cell. 2006; 21:337–347. [PubMed: 16455489]

48. Mackinnon AC, Qadota H, Norman KR, Moerman DG, Williams BD. C. elegans PAT-4/ILK functions as an adaptor protein within integrin adhesion complexes. Curr Biol. 2002; 12:787–797. [PubMed: 12015115]

49. Das M, Ithychanda SS, Qin J, Plow EF. Migfilin and filamin as regulators of integrin activation in endothelial cells and neutrophils. PLoS One. 2011; 6:e26355. [PubMed: 22043318]

50. Riveline D, Zamir E, Balaban NQ, Schwarz US, Ishizaki T, Narumiya S, Kam Z, Geiger B, Bershadsky AD. Focal contacts as mechanosensors: externally applied local mechanical force induces growth of focal contacts by an mDia1-dependent and ROCK-independent mechanism. J Cell Biol. 2001; 153:1175–1186. [PubMed: 11402062]

51. Grashoff C, Hoffman BD, Brenner MD, Zhou R, Parsons M, Yang MT, McLean MA, Sligar SG, Chen CS, Ha T, Schwartz MA. Measuring mechanical tension across vinculin reveals regulation of focal adhesion dynamics. Nature. 2010; 466:263–266. [PubMed: 20613844]

52. Kong F, Garcia AJ, Mould AP, Humphries MJ, Zhu C. Demonstration of catch bonds between an integrin and its ligand. J Cell Biol. 2009; 185:1275–1284. [PubMed: 19564406]

53. Miyamoto S, Akiyama SK, Yamada KM. Synergistic roles for receptor occupancy and aggregation in integrin transmembrane function. Science. 1995; 267:883–885. [PubMed: 7846531]

54. Sastry SK, Burridge K. Focal adhesions: a nexus for intracellular signaling and cytoskeletal dynamics. Exp Cell Res. 2000; 261:25–36. [PubMed: 11082272]

55. Bunch TA. Integrin alphaIIbbeta3 activation in Chinese hamster ovary cells and platelets increases clustering rather than affinity. J Biol Chem. 2010; 285:1841–1849. [PubMed: 19917607]

56. Ye F, Petrich BG, Anekal P, Lefort CT, Kasirer-Friede A, Shattil SJ, Ruppert R, Moser M, Fassler R, Ginsberg MH. The mechanism of kindlin-mediated activation of integrin alphaIIbbeta3. Curr Biol. 2013; 23:2288–2295. [PubMed: 24210614]

Highlights

- α-Actinin clusters transiently associate with integrin as adhesions form
- Integrin associates with kindlin but not talin during adhesion assembly
- Integrin-talin complex forms in response to myosin II activity as adhesion mature
- The ratio of molecules differs in nascent versus focal adhesions

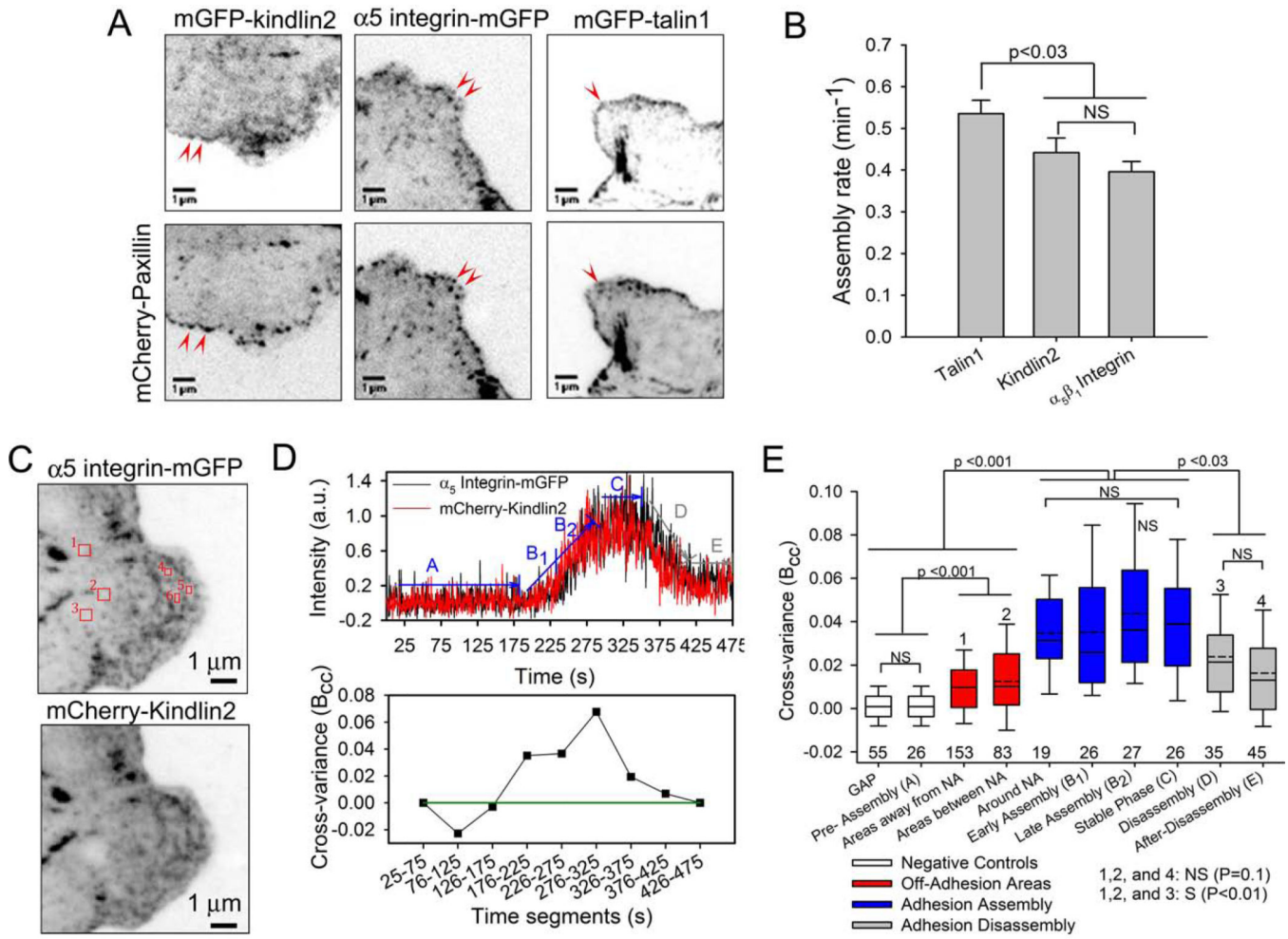

Figure 1. Cross-variance of $\alpha_5\beta_1$ integrin and kindlin2 in nascent adhesions

(A) α_5 integrin co-localizes with talin1, and kindlin2 in nascent adhesions (arrows) with (B) variable assembly rates in CHOK1 cell co-transfected with mCherry-paxillin and the designated GFP tagged plasmid. (C) TIRF images (average over 50 seconds) of α_5 integrin-mGFP and mCherry-kindlin2 used for cross-variance analysis. (D) Fluorescence intensity time trace of α_5 integrin-mGFP and mCherry-kindlin2 in a selected nascent adhesion and the corresponding cross-variance (B_{cc}) values calculated from phases of adhesion formation and disassembly (labeled A-E). (E) Box plot of the (B_{cc}) values from pixel regions corresponding to both adhesions and regions without adhesions. (B_{cc}) values calculated from areas away (N=17) and between (N=19) adhesions were averaged over 5x5 and 3x3 pixel regions respectively. For areas between adhesions, (B_{cc}) values corresponding to time segments when no adhesions were visible yet were discarded. (B_{cc}) values for regions around adhesions were calculated from single square pixel regions surrounding the adhesion. GAP (GAP-mGFP and GAP-mCherry) constitute a negative control. Images were acquired every 500 ms.

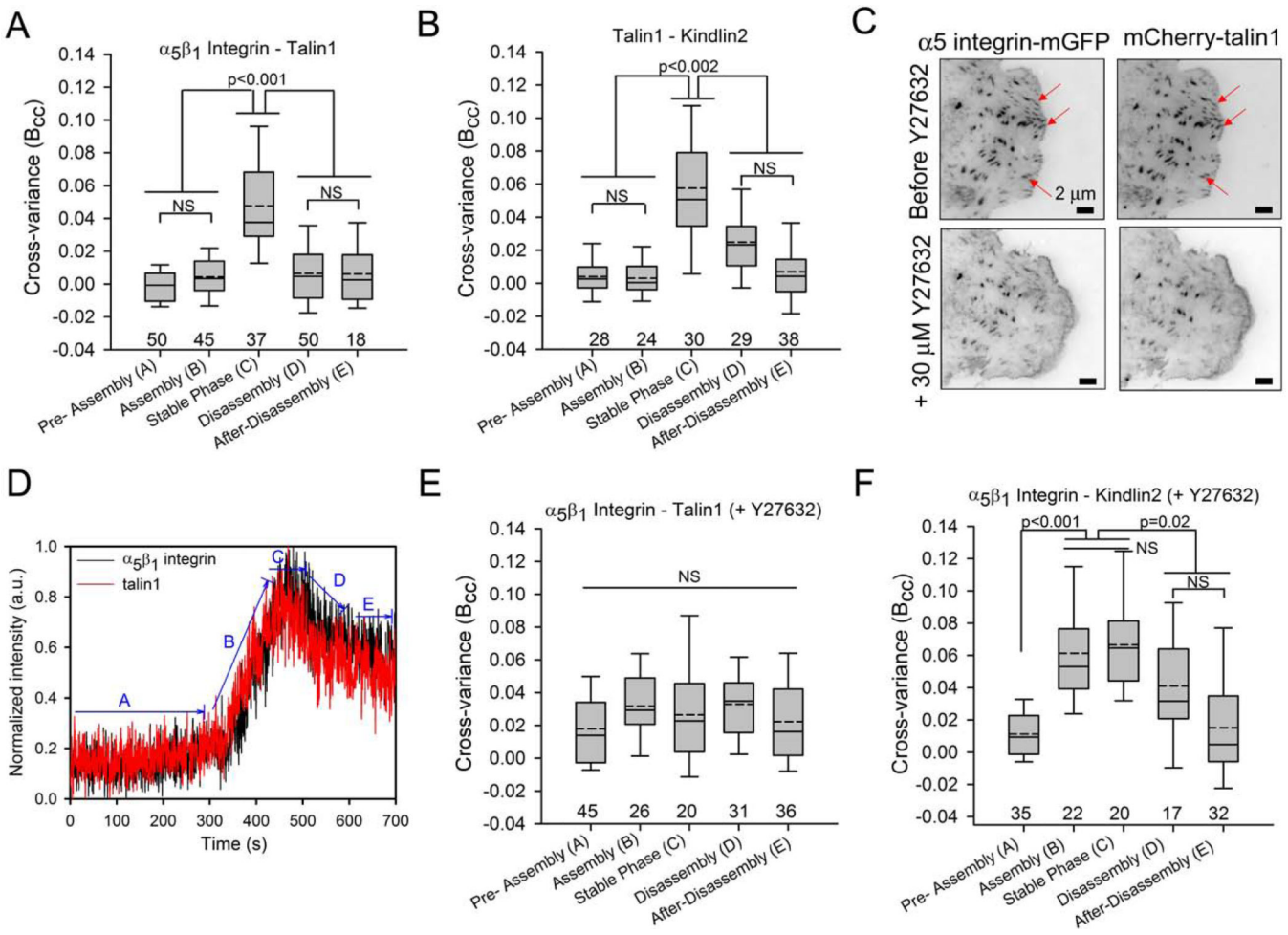

Figure 2. Cross-variance of talin-$\alpha_5\beta_1$ integrin, and talin-kindlin2 in nascent adhesions

Box plots of (B_{cc}) values calculated for phases of nascent adhesion formation in CHOK1 cells expressing (A) $\alpha_5\beta_1$ integrin-mGFP and mCherry-talin1 and (B) mGFP-talin1 and mCherry-kindlin2. (C) Intensity images (averaged over 3 min) of U2OS cells expressing $\alpha_5\beta_1$ integrin-GFP and mCherry-talin1 before and 8 min after treatment with Y27632 drug; (D) note the $\alpha_5\beta_1$ integrin-mGFP and mCherry-talin1 containing nascent adhesions do not mature into larger adhesions similar to those highlighted by arrows in (C). (E) Box plot of (B_{cc}) values measured from nascent adhesions in cells treated with Y27632 drug show abolished associations between $\alpha_5\beta_1$ integrin-mGFP and mCherry-talin1, but not between (F) $\alpha_5\beta_1$ integrin-mGFP and mCherry-kindlin2. Images were acquired every 500 ms.

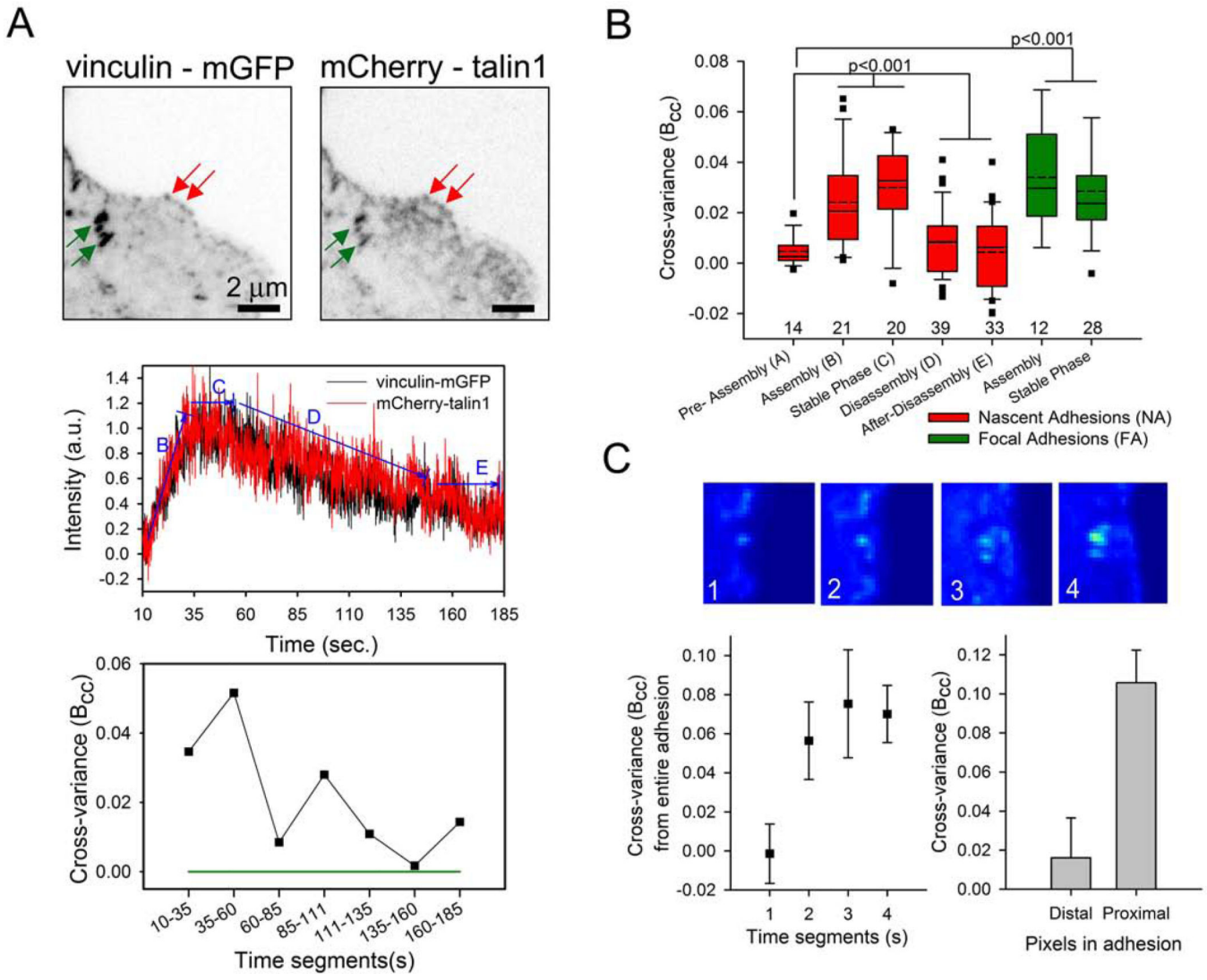

Figure 3. Cross-variance of talin1 and vinculin in adhesions

(A) Vinculin-mGFP and mCherry-talin1 localize to nascent (NA) and focal adhesions (FA) in CHOK1 cells. (B) Representative fluorescence time traces and (B_{cc}) values for vinculin-mGFP and mCherry-talin1 in a nascent adhesion that disassembles. (B) Box plot of the (B_{cc}) values calculated at different times during nascent adhesion formation and from adhesions that stabilize into larger focal adhesions (FA), inferring that they reside in a common complex. The (B_{cc}) values for the pixels corresponding to individual FA's (N=5) were averaged over the time segments. (C) Images from selected time segments in the vinculin time series depict the formation of a nascent adhesion that matures into a focal adhesion by elongating perpendicular to the direction of the protrusion. Different (B_{cc}) values at the distal versus proximal regions relative to the protrusion suggest a differential exchange of the molecular complex in different regions of the elongating adhesion.

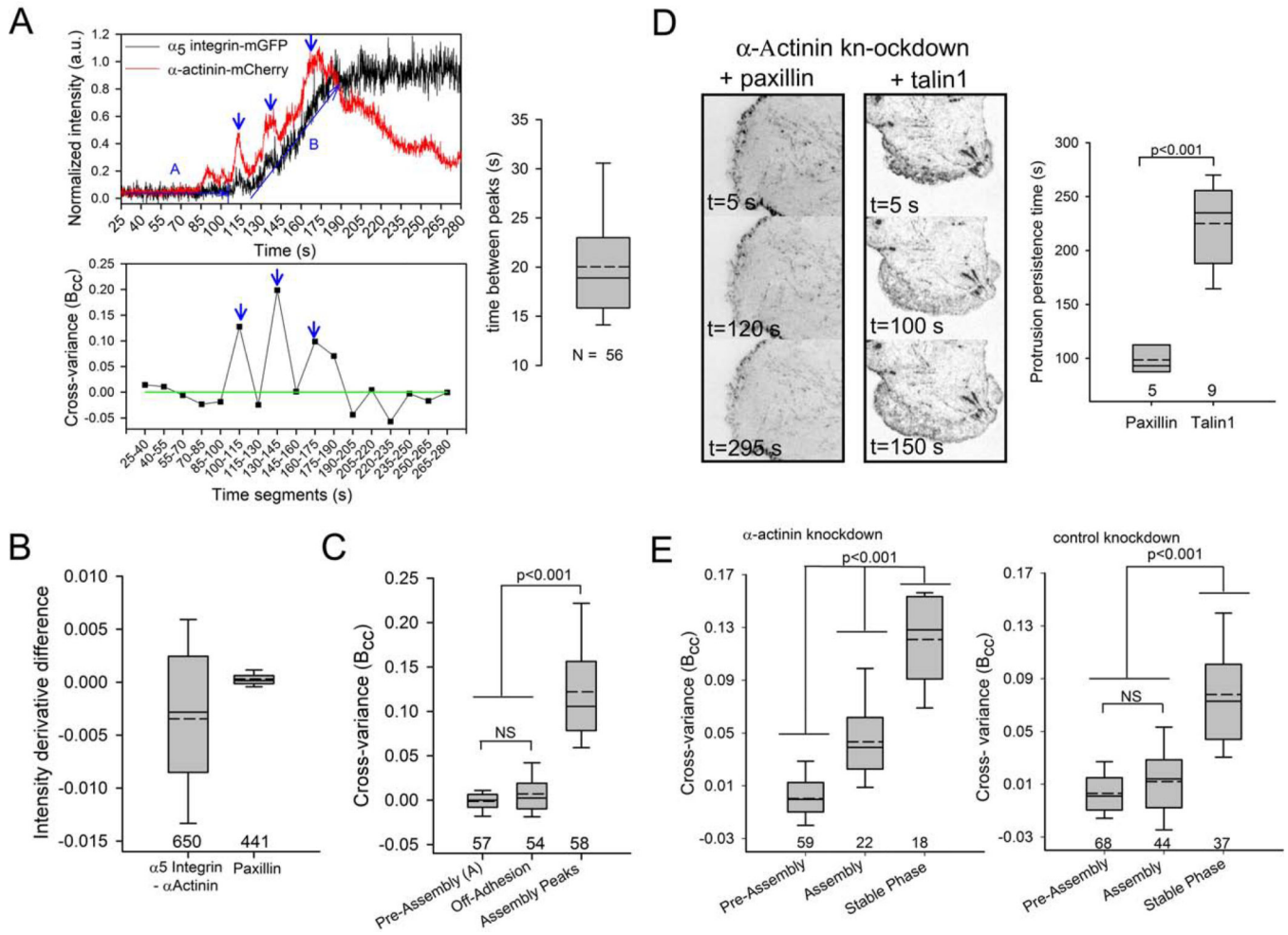

Figure 4. $\alpha_5\beta_1$ integrin and α-actinin assembly and association in nascent adhesions

(A) Intensity time trace of α_5 integrin-mGFP and α-actinin-mCherry in a nascent adhesion in CHOK1 cells. Arrows show α-actinin intensity spikes during assembly and the average duration between the intensity spikes. (B) The difference in the intensity derivative during assembly for α_5 integrin-mGFP and α-actinin-mCherry, in comparison to mCherry-paxillin-GFP, indicates that α-actinin assembles at a faster rate relative to $\alpha_5\beta_1$ integrin. (C) High positive (B_{cc}) values correspond to the α-actinin intensity peaks during nascent adhesion assembly, whereas no cross-variance is detected in pixels corresponding to regions between adhesions (Off-adhesions). 25 adhesions were used for quantifications in (A-C). (D) α-actinin knockdown in CHOK1 cells expressing talin1-mGFP and mGFP-paxillin. In contrast to paxillin, cells expressing talin1 show persistent protrusive activity. (E) Effect of α-actinin knockdown on the association of $\alpha_5\beta_1$ integrin and talin1 during nascent adhesion formation. For cross-variance analysis, images were acquired every 100 ms for mCherry-paxillin-mGFP, 150 ms for integrin-α-actinin, and 500 ms for integrin-talin1.

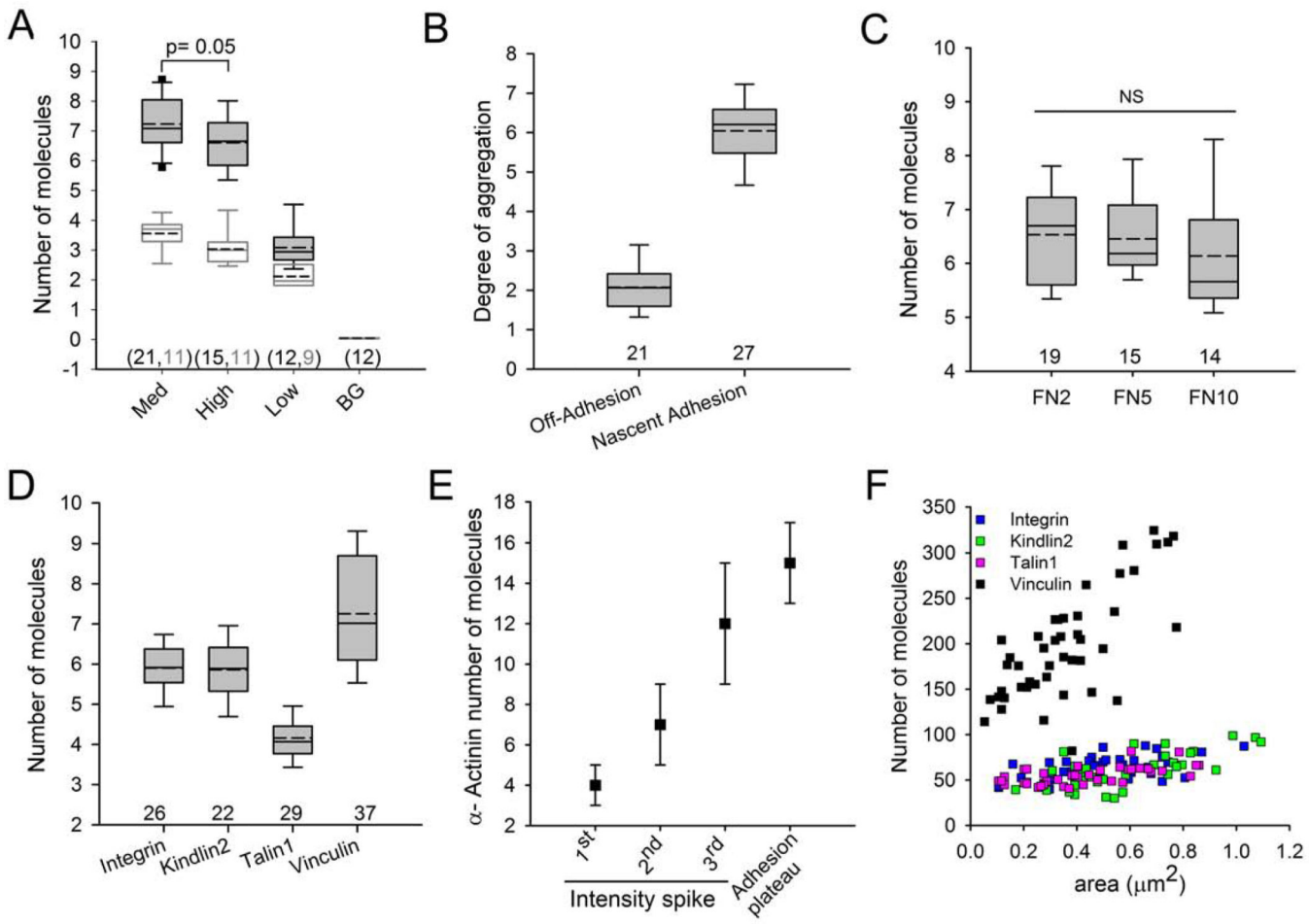

Figure 5. The number of $\alpha_5\beta_1$ integrins and its partners in adhesions

(A) Number of molecules of $\alpha_5\beta_1$ integrin as a function of expression level in nascent adhesions that stabilize. Expression level is classified based on the average intensity of $\alpha_5\beta_1$ integrin in protruding regions of CHOB2 cells, which lack endogenous $\alpha_5\beta_1$, stably expressing ectopic α_5 integrin-mGFP. (B) Degree of aggregation of $\alpha_5\beta_1$ integrin in nascent adhesions. (C) Number of molecules of $\alpha_5\beta_1$ integrin as a function of variable fibronectin coating concentrations. Number of molecules of $\alpha_5\beta_1$ integrin, kindlin2, talin1, and vinculin in (D) nascent and (E) focal adhesions (as a function of size). (F) α-actinin numbers in nascent adhesions and in the intensity peaks that form during assembly selected from 25 adhesions (see Figure 4). The step size of the α-actinin spikes was measured as the difference between the peak intensity of the n^{th} spike and the trough intensity of the $(n-1)^{th}$ peak. For the first intensity peak, we used the pre-assembly intensity levels to determine the step size.